Models of scattered light in UXORs

A. Natta[1] and B.A. Whitney[2]

[1] Osservatorio Astrofisico di Arcetri, Largo E. Fermi 5, 50125 Firenze, Italy
[2] Space Science Institute, 3100 Marine St., Suite A353, Boulder, CO 80303-1058, USA

Abstract. This paper offers an interpretation of the photometric and polarimetric variability of UXORs where the star is surrounded by an optically thick, flared circumstellar disk similar to pre-main–sequence disks. A screen of dust sporadically obscures the stellar radiation, causing a minimum of the stellar light. Using a Monte Carlo code developed by Whitney & Hartmann (1992) we compute the polarization and colors of the observed radiation, and compare it to the available observations. The agreement is remarkably good. We find that the UXOR phenomenon occurs for systems seen in a well-defined range of inclinations, roughly between 45° and 65°–68°. About 1/2 of the optically visible Herbig Ae stars should be UXORs, i.e., have deep photometric minima accompanied by a large increase in the polarization fraction, provided that screens can form. The results are not sensitive to the disk parameters, as long as the disk intercepts about 20% of the stellar radiation. The screens causing the light minima have sizes of the order of 1–few stellar radii, optical depth $\tau_V \sim$ 3–5, and contain relatively small grains. We find a good fit to the observations with a MRN distribution with average radius $\sim 0.03\,\mu$m. The lack of UXORs with low polarization in deep minima can be understood if the screens are confined in a region close to the disk plane. However, the nature and origin of the screens remain open questions.

Key words: stars: pre-main sequence – stars: circumstellar matter – stars: variables: general

1. Introduction

UXORs are defined as pre-main–sequence stars of intermediate mass, mostly Herbig Ae (HAe) stars, characterized by large and irregular variability. At visual wavelengths, they show sporadic deep minima, when the star fades by as much as 2–3 magnitudes. As the star fades, its colors become first redder, approximately following the expectations for dust extinction; however, when the star is close to minimum light, one often observes a color reversal (called "blueing"). The decrease of the stellar light is accompanied by a simultaneous increase of the fraction of polarized light seen by the observer. These phenomena are described

in a number of papers, reviewed most recently in Waters & Waelkens 1998, Herbst & Shevchenko 1999, Grady et al. 2000, Natta et al. 2000.

The most widely accepted interpretation of such phenomena (but see Herbst & Shevchenko 1999) is in terms of a star+disk system, seen almost edge-on. A minimum in the observed light is caused by a clump of dust which suddenly intercepts the line of sight to the observer and obscures the stellar light. At minimum, the observer only sees radiation scattered by the disk into the line of sight, which is therefore bluer and more polarized than the unshielded radiation from the star+disk system (e.g., Grinin 1992). It has been argued that the dust clouds may contain asteroid-sized bodies (see, for example, Friedemann et al. 1995).

The properties of the UXORs photopolarimetric variability have been studied by modeling the disk as a large, ellipsoidal optically thin cloud of grains (Voshchinnikov et al. 1988, 1995; Voshchinnikov & Grinin 1991; Krivova & Il'in 1997, 2000). However, recent interferometric millimeter observations of some UXORs (CQ Tau, UX Ori and WW Vul) (Mannings & Sargent 1997, 2000; Natta et al. 1997, 1999) and the analysis of theoretical SEDs in the IR and millimeter ranges (Natta et al. 1999) have shown that these stars are surrounded by circumstellar disks similar to those associated with T Tauri stars (TTS): flared, optically thick, with mass 0.01–0.1 $M_\odot$.

We present in this paper models of UXORs where we assume that the circumstellar disk has the properties of a typical pre-main–sequence disk, as inferred from the SEDs. We will discuss the predicted behaviour of the visual colors and polarization of the observed radiation as the star is occulted by an intervening clump of dust, and show that these models can account perfectly well for the observations.

2. Models

Let us consider a star and disk system. The disk absorbs and scatters the stellar radiation, so that the observed flux at any wavelength where the disk emission is negligible is just the sum of the direct stellar light not intercepted by the disk plus that scattered by the disk into the direction of the observer. This fraction depends on the disk geometrical properties, its inclination with respect to the line of sight, and on the kind of grains on the disk surface. Unless the disk is seen exactly face-

on and is uniformly illuminated, the scattered light is polarized, and so is the observed flux.

We describe the UXORs variability assuming that at some instant in time a fraction f of the stellar surface is obscured by a screen of optical depth τ_λ, so that the light received by the observer is given by:

$$F_{obs} = F_\star (1 - \epsilon) \left[1 - f(1 - e^{-\tau_\lambda}) \right] + F_{scat} \qquad (1)$$

where ϵ is the fraction of the stellar radiation intercepted by the disk. The observed flux at maximum light ($\tau_\lambda=0$) is equal to

$$F_{obs}^{max} = F_\star (1 - \epsilon) + F_{scat}. \qquad (2)$$

The effect of the screen is to decrease the amount of direct stellar light (and therefore the total flux), thus increasing the fraction of scattered light received by the observer, and as a consequence, also the observed polarization.

The calculations have been performed using the code described in Whitney & Hartmann (1992), but modified to use the exact phase function of the adopted dust rather than the commonly used Henyey-Greenstein approximation for phase function. This is done by sampling from tables of the 8-element scattering matrix (for spheres in this case) using the rejection method. Rotations of the scattering matrix in and out of the scattering frame are performed as in Code & Whitney (1995).

The model requires us to define a number of parameters, and we have proceeded in the following way: we have considered a star of $\sim 2\,M_\odot$, $L_\star \sim 50\,L_\odot$, $T_\star \sim 9000\,K$ (early A spectral type) surrounded by an optically thick circumstellar disk extending from the dust sublimation radius R_i ($\sim$ few $R_\star$ for the adopted stellar parameters) to an outer radius R_D. The disk is flared due to its thermal pressure; following Chiang & Goldreich (1997; in the following CG97), we describe the height of the disk photosphere as:

$$H/R_\star \sim \zeta_\star (R/R_\star)^{9/7} \qquad (3)$$

with $\zeta_\star$ the height of the disk (in units of $R_\star$) at the fiducial radius $R_\star$. The combination of the flaring exponent and the assumed height of the disk, $\zeta_\star$, determines the amount of flux scattered from the disk. In our reference (standard) models, we have assumed $\zeta_\star$=0.032, as appropriate for the adopted stellar parameters (CG97), R_i=4 $R_\star$, R_D=100 AU, surface density $\Sigma \propto R^{-1.5}$, and we have considered two disk masses $M_D = 0.01$ and 0.1 $M_\odot$. Disks in this mass range account for the observed millimeter fluxes of most UXORs (Natta et al. 1997, 1999). In Sect. 3, we will briefly discuss the dependence of the results on the adopted disk model.

The dust on the disk surface is made of small grains, with properties similar to those of grains in the ISM (Mathis et al. 1977, MRN; Kim et al. 1994). We summarize their properties in Fig. 1. In fact, it is possible that some grain growth has occurred on the disk surface of UXORs (Reimann et al. 1997; Natta et al. 1999), and we will come back to this point in Sect. 4.

It is not the purpose of this paper to investigate the nature of the screen. Here we only need to specify two properties, one is the fraction f of the stellar surface covered by the screen and the
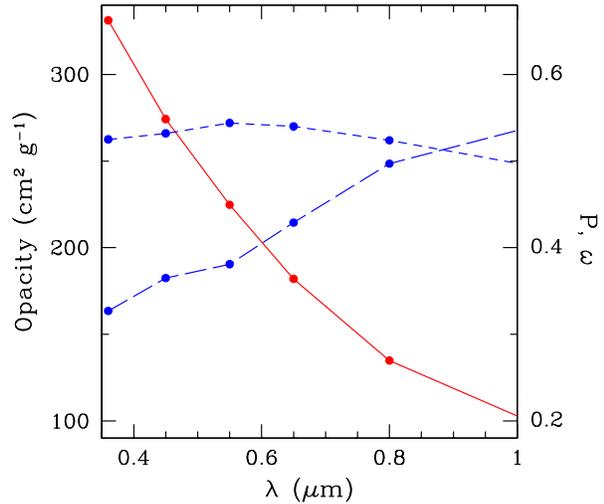
Fig. 1. Dust properties. Plotted as function of λ are the adopted opacity (scattering+absorption; solid line), the albedo ω (short-dashed line) and the maximum polarization which occurs at roughly a 90° scattering angle (long-dashed line).

second is the screen optical depth as a function of wavelength. In our main grid of models, we have assumed that the screen covers the entire stellar surface (but not the disk), and that the grains in the screen are similar to those in the surface layers of the disk. We will comment on these assumptions in Sect. 4.

For each value of the screen optical depth, we have computed ΔV, i.e., the variation of the observed V magnitude with respect to the unobscured case (see Eq. (2)), the fraction of polarization P in the five photometric bands U,B,V,R,I and the color excesses Δ(U-B), Δ(B-V), Δ(V-R), Δ(V-I). The reference magnitudes in all bands are those of the unoccluted system, i.e., observed at maximum light. The stellar properties do not affect directly the polarization fraction, nor the color excess. When computing color-magnitude diagrams for individual stars (see Sect. 3), we have used as reference the observed magnitudes of the star at maximum.

The contribution of the screen to the amount of scattered light we receive is not taken into account in our models. If the screen is a roughly spherical cloud of particles, we show in the Appendix that unless it is very large, it will scatter in the most favorable situation an order of magnitude less flux than the disk. Thus, ignoring its effect should not change the nature of our results. If there is not one or few clumps only, but many ($\gtrsim$50), their contribution to the scattered light may become significant and should be taken into account. We defer a further discussion of this possibility to a forthcoming paper.
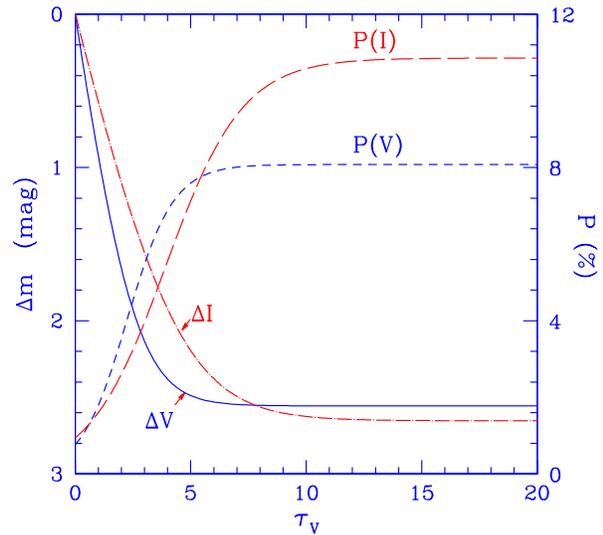
3. Results

The main result of our calculations is shown in Fig. 2. This figure plots the predicted fraction of polarized radiation (in the V band) received by the observer as the star is occulted by a screen of increasing optical depth. Each curve corresponds to a different inclination angle of the disk with respect to the observer, from almost face-on ($\theta = 13^o$) to $\theta = 68^o$. Larger θ have to be ruled
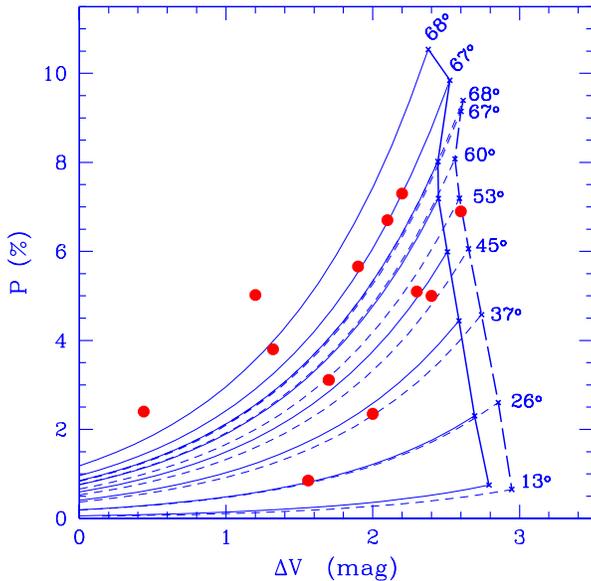
Fig. 2. This figure plots the values of the polarization fraction in the V band as function of the brightness variation ΔV caused by a screen of increasing optical depth intercepting the stellar light. To the right, the two roughly vertical lines show model predictions for different disk masses (0.01 M$_\odot$, dashed line, and 0.1 M$_\odot$, solid line) when the stellar light is completely blocked by the screen, i.e., when only the scattered light reaches the observer. Along each (vertical) line, the inclination of the disk with respect to the line of sight varies from 13° (face-on) to 68° (edge-on), as labelled. For larger inclinations (not plotted), the outer disk intercepts the line of sight to the star. As ΔV decreases, i.e., as the fraction of stellar radiation received by the observer gets larger, the points move to the left, as shown by the thin solid and dashed lines. The dots show the observed points (see text). Each corresponds to a star, seen at its minimum light.


Fig. 3. ΔV (solid line), ΔI (dot-long-dashed line), $P(V)$ (short-dashed line) and $P(I)$ (long-dashed line) as function of the cloud optical depth τ_V. The disk is the reference CG97 disk with M_D=0.1 M$_\odot$, seen at an inclination θ=60°.

out, since the outer disk will begin to obscure the star causing an extinction much larger than that observed in UXORs ($\lesssim$ 1–2 mag). When the star is not occulted by the screen (ΔV=0), the fraction of polarized light is minimal. Its value is proportional to the contribution of light scattered by the disk in the direction of the observer, and depends on the disk inclination, being larger for more edge-on systems. However, it is never larger than $\sim$1%. As the star fades due to the screen, the relative contribution of the scattered light increases. The polarization also increases until it reaches a maximum value which, for $\theta \gtrsim 60^o$, is of the order of 8–9%. For any given θ, there is a *maximum* value, which corresponds to a situation where only scattered light reaches the observer. Increasing further the optical depth of the screen does not cause further changes in P or ΔV. The asymptotic behaviour of P and ΔV with the clump optical depth is illustrated in Fig. 3. Note that $\Delta V \gtrsim 2.5$ mag requires a rather large value of τ, in this particular example $\tau_V \gtrsim 4$.

The dots in Fig. 2 show the observed values of the V polarization fraction as function of ΔV in deep minima for those HAe stars for which simultaneus photopolarimetric observations exist in the literature. Each point refers to one star and plots the value of P observed in its deepest minimum. Most of the data come from the monitoring program carried on at

the Crimean Astrophysical Observatory (Grinin 1994; Grinin & Rostopchina 1996 and references therein); in a few cases we have re-estimated the value of ΔV from the original sources, and we have added more recent data from the literature for the less massive star BM And (spectral type F8; Grinin et al. 1995) and for RR Tau (Rostopchina et al. 1997). When several minima of similar ΔV have been observed, we plot the average of P. In general, the dispersion is small, less than 1% in P and 0.1–0.2 mag in ΔV. Note that the values of maximum decline ΔV can be underestimated, especially if only short time sequences are available. However, this is not the case for most of the stars plotted in Fig. 2, for which we can be quite confident that deeper minima can be ruled out.

The observations are well accounted for by the models. No observational point lies to the right of the vertical lines, a region which, as discussed above, is forbidden in these models. Most stars are accounted for by models with inclination lower than $\sim 68^o$. More precisely, 8 out of 12 stars require disks with inclination roughly between 45° and 68°. We will come back to this point and its implications in the following section.

Fig. 4 shows the dependence of the results on disk parameters. We have varied the inner disk radius $R_i = 4$–22 R$_\star$, the outer disk radius $R_D = 50$–200 AU, the surface density profile ($\Sigma \propto R^{-1.0}$, $\propto R^{-1.5}$, $\propto R^{-2.0}$) and the disk mass ($M_D = 0.01$ and 0.1 M$_\star$; see Fig. 2). The results are easily understood if we consider that the maximum ΔV depends only on the fraction of stellar light that is intercepted and scattered by the disk. For any given value of θ, ΔV decreases for higher disk mass, larger outer radius and flatter Σ because more light is scattered from these disks. The maximum value of P, in contrast, does not depend on the fraction of scattered light, but only on the relative contribution to it from different parts of the disk, which scatter light at slightly different position angles. In
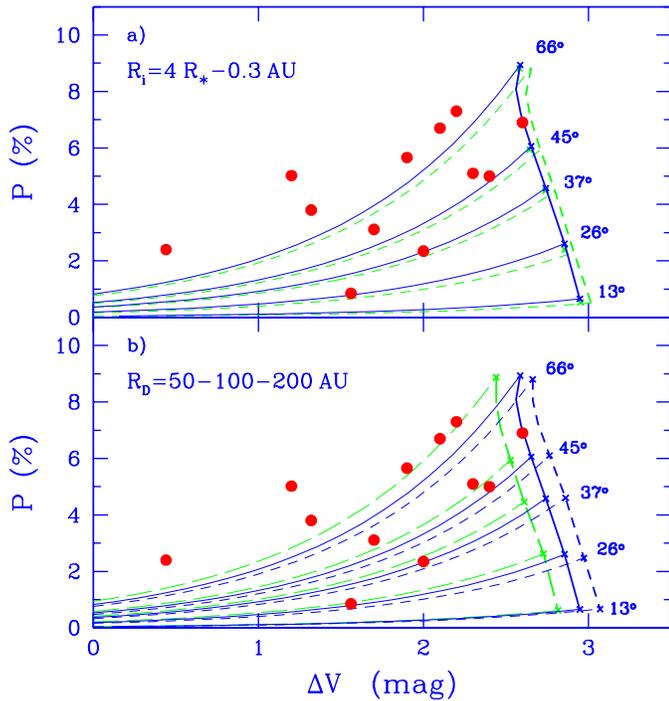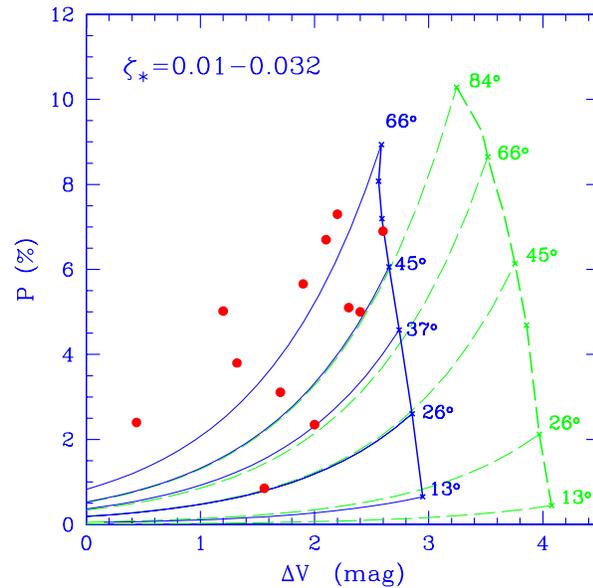
Fig. 4a and b. Same as Fig. 2 for different disk models. In all panels the solid lines show the predictions of a model with M_D=0.01 M$_\odot$, R_i=4 R$_\star$, R_D=100 AU, $\Sigma \propto R^{-1.5}$, $\zeta_\star$=0.032. The dashed lines show models where we have changed one parameter at the time: In Panel **a** R_i=22 R$_\star$, in Panel **b** R_D=50 (short-dashed) and 200 (long-dashed) AU. In all cases M_D=0.01 M$_\odot$.

our models, light scattered by the outer disk, where the position angle of the polarization causes some cancellation, is less polarized than light scattered by the inner disk; therefore P decreases slightly with increasing M_D and R_D and flatter Σ. There is also a small dependence of ΔV and P on R_i, as disks with larger inner radius scatter slightly less stellar radiation. The difference is small because the disk wall at the inner radius intercepts most of the stellar radiation that would have hit the surface if the inner radius were smaller. The flux from the wall is less polarized however, than if it had hit the disk surface. Inspection of Figs. 2 and 4 (the results for different Σ are practically identical and are not shown) shows that many different sets of disk parameters, within the range we have explored, can account equally well for the observations.

The only critical parameter is the fiducial disk height, as shown by Fig. 5, where we compare models with $\zeta_\star$=0.032 and 0.01. The small $\zeta_\star$ disk intercepts significantly less stellar light, so that the maximum ΔV for any given θ is about 1 mag larger.

In order to further check the capability of the disk models to explain the overall behaviour of UXOR minima, and not only the observed relation of the maximum value of P with ΔV, we have computed the dependence of the polarization fraction on wavelength. Fig. 6 shows in Panel a) the results for the standard CG97 disk of mass M_D=0.1 M$_\odot$, seen at an inclination of 60°, as the star fades i.e., for increasing values of ΔV. The curve labelled ΔV=2.4 mag corresponds to the case when the stel-


Fig. 5. Same as Fig. 2 for different disk height $\zeta_\star$. Solid lines refer to $\zeta_\star$=0.032, dashed lines to $\zeta_\star$=0.01. The other disk parameters are M_D=0.01 M$_\odot$, R_i=4 R$_\star$, R_D=100 AU, $\Sigma \propto R^{-1.5}$. Note that for $\zeta_\star$=0.01, θ can be much larger than $\sim 66^o$ before the outer disk begins to obscure the star.

lar radiation is completely absorbed at all wavelengths ($\tau_V \gtrsim$ 10; see Fig. 3) and the dependence of P on λ reflects the dust properties. For the adopted ISM grains, the polarization of the scattered light increases with wavelength roughly as a power-law of slope ~ 0.43. As ΔV decreases, the observer sees a larger fraction of unpolarized stellar radiation, which increases with wavelength due to the reddening caused by the screen: the polarization decreases at all wavelengths, and its slope becomes negative. In this particular disk model, for example, for $\Delta V = 1.7$ mag the slope is ~ -0.53. When the star is not occulted at all (ΔV=0), the residual small polarization again has a positive slope ($\propto \lambda^{0.33}$).

The transition from positive to negative slopes occurs for a very small change in ΔV (~ 0.1 mag), which, however, corresponds to a large variation in τ_V, from ~ 10 to ~ 4 (see Fig. 3). In this particular example, while for τ_V=10 we observe only scattered light at all wavelengths, for τ_V=4 there is a contribution of 13% from unpolarized stellar radiation in V and of 45% in I.

The other three panels show observations for three representative UXORs, namely UX Ori, WW Vul and CQ Tau at different epochs. At least qualitatively, the behaviour is in agreement with model predictions. Note that while the run of P with λ is sensitive to the grain properties, it does not depend much on disk parameters such as flaring, mass, etc. Changing the inclination affects the values of P at all wavelengths, but almost insignificantly its dependence on wavelength. Of the three stars in Fig. 6, we find the best agreement between observations and models for inclinations $\theta = 53^o$ for WW Vul, $\theta = 60^o$ for UX Ori and $\theta = 66^o$ for CQ Tau.
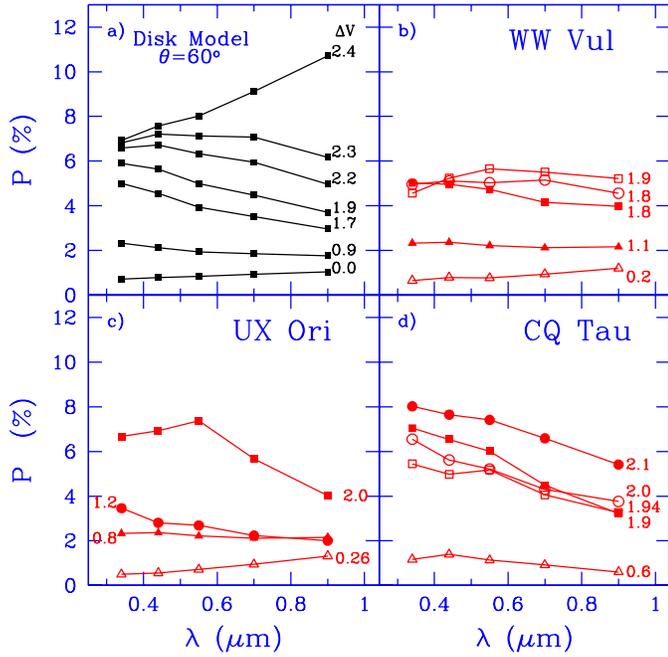
Fig. 6a–d. Polarization fraction as function of wavelength for the 5 bands U,B,V,R,I. Panel **a** shows model predictions for the CG97 standard disk, $M_D = 0.1\,M_\odot$, seen at an inclination angle of 60°. Curves from bottom to top correspond to increasing values of ΔV, as labelled. Panels **b**, **c** and **d** show the observed values of P vs. λ for the stars WW Vul, CQ Tau, UX Ori seen at various ΔV, as labelled. Data are from Berdyugin et al. 1992 (WW Vul), Voshchinnikov et al. 1988 (UX Ori), Berdyugin et al. 1990 and Berdyugin 1993 (CQ Tau), respectively.
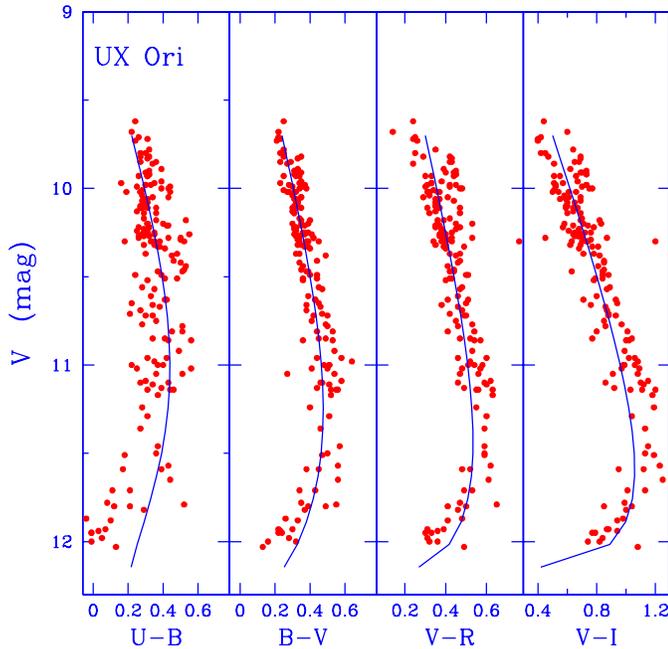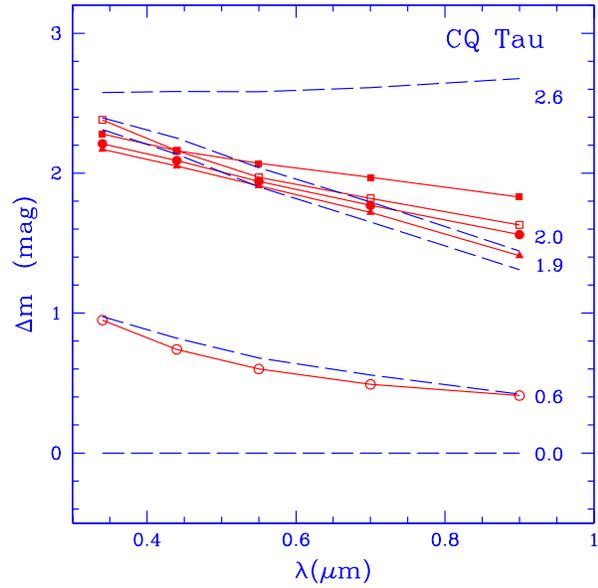
Fig. 8. Photometric variation of CQ Tau at various epochs as function of λ. The variation is measured with respect to the bright state (Berdyugin 1993). The dashed curves plot model predictions for the a disk with $M_D = 0.01\,M_\odot$, $R_i = 10\,R_\star$, $R_D = 100$ AU, $\zeta_\star = 0.032$, $\theta = 66^o$. Labels to the right refer to the model ΔV. For $\Delta V = 2.4$ mag only scattered light reaches the observer at all wavelengths. The observed ΔV can be read from the figure.

A good agreement between models and observations is shown also by the UX Ori magnitude-color plot of Fig. 7. The dots show the observational data from the Crimea Observatory database, and the curves are predictions of a disk model with parameters specified in the figure caption. Note the well-known "blueing" effect, which characterizes the minima of UXORs. Finally, we show in Fig. 8 the dependence on wavelength of the photometric variation observed at different epochs in CQ Tau (Berdyugin et al. 1990; Berdyugin 1993) and compare it with model predictions. Again, the agreement is rather good.

4. Discussion

4.1. Grain properties

The results discussed in Sect. 3 depend somewhat on the assumed dust properties. Dust on the disk surface determines the fraction of stellar light scattered and polarized at the various wavelengths, while dust in the obscuring screen determines the dependence on wavelength of the fraction of stellar light that reaches the observer directly. The dependence on wavelength of P and Δm observed in UXORs minima can be used to constrain grain properties, once the geometry of the system is known. Although a detailed analysis of the required grain properties is beyond the scope of this paper, we want to stress here two points.

The first is that the observed colors of the radiation as the star fades (see Figs. 7 and 8) are not consistent with a dominant population of large grains ($\gtrsim 1\,\mu m$) in the occulting screen, which would cause a grey extinction. Some deviation from a MRN dis-

Fig. 7. Color-magnitude diagrams for UX Ori. The observed points are from the database of the Crimean Astrophysical Observatory, kindly provided to as by A. Rostopchina. The solid lines show the model predictions. The disk has $M_D = 0.1\,M_\odot$, $R_i = 4\,R_\star$, $R_D = 100$ AU, $\zeta_\star = 0.032$, $\theta = 60^o$.

tribution, slightly varying from star to star and between different minima, is however likely. Voshchinnikov et al. (1995) find that a MRN grain distribution with grain sizes roughly between 0.05 and 0.15–0.25 μm fits well the color-magnitude behaviour of UX Ori and WW Vul (see also Friedemann et al. 1993).

The second point concerns the properties of the dust on the surface of the disk. The radiation scattered by large grains ($\gtrsim 1\,\mu$m) has a wavelength-independent polarization fraction, as observed, for example, in β Pic (Gledhill et al. 1991; Wolstencroft et al. 1995). If we consider individual UXORs, we cannot exclude the existence of large grains on the surface of the disk, as long as the optical depth of the obscuring cloud decreases with increasing wavelength. On a statistical basis however, we note that large grains have lower scattering cross section and polarizability, so that for any given set of disk parameters and orientation the maximum value of ΔV is larger and P is lower than for smaller grains. The agreement between P and ΔV observed in the deep minima of UXORs, which is remarkably good for small grains (see Fig. 2), disappears. In fact, given that the timescales for grain settling to the disk midplane are longer for smaller grains, it is expected that only the smallest grains remain suspended in the upper layers where the stellar radiation is scattered (Ruden 2000 and references therein). Thus our use of the ISM Kim et al. (1994) grain model may not be such a bad approximation in this initial exploration. However, it comes as a surprise that the models fit as well as they do, indicating that the grains are not significantly larger than $0.1\,\mu$m.

4.2. Disk properties

As discussed in Sect. 3, detailed disk properties are not strongly constrained by the observations, as long as a significant fraction of the stellar radiation is intercepted by the disk. We can estimate the fraction of scattered light to be $\sim$10% from the maximum depth of the minima, which is of the order of 2.5 mag. For an albedo of $\sim$0.5, this means that the disk must intercept about 20% of the stellar radiation, a very reasonable value for many flared disk models, even when the disk has a large inner hole.

In the CG97 models, most stellar light is intercepted at large radii and the contribution of the inner disk to the observed scattered radiation is negligible. It is however possible that the inner disk is more flared than in our assumptions (see, for example, Bell et al. 1997 and Bell 1999). Such an inner bulge can happen on the 10–20 AU scale and, if optically thick, will obscure most of the outer disk. However, we do not expect any major change in our results, as long as the fraction of the stellar radiation intercepted and scattered remains similar. This possibility needs to be explored further, since it may have interesting implications for the nature of the obscuring screens.

4.3. Disk orientation

The results of Fig. 2 show that most UXORs can be explained by disks seen at an inclination angle of $\sim 45^o - 68^0$. This is significantly less edge-on than required by models where the scatterers have an ellipsoidal distribution around the star. For example, we

can fit well the data for WW Vul for $\theta \sim 53^o$, while Krivova & Il'in (2000) propose $\theta \sim 75^o$. This result supports strongly our hypothesis that UXORs are associated with "normal" pre-main–sequence disks. If a larger inclination was required, we would run into the problem that at $\theta \gtrsim 65^o - 68^o$ (depending on the disk model) the outer layers of the disk obscure the star at all times (see, for example, Chiang & Goldreich 1999). This is not observed, since UXORs at maximum light have typical extinction $\lesssim$1 mag (van den Ancker et al. 1998).

If we consider that stars obscured by the outer disk will not be classified as Herbig Ae stars, because they are not optically visible, we expect to have 50% of HAe with disk inclination between 0° and 45°, and 50% between 45° and 67°, assumed as the limiting value of θ. The inclination angle distribution of known UXORs is skewed towards large inclinations, with 10/12 stars at $\theta \gtrsim 45^o$ and only 2/12 at $\theta \lesssim 45^o$. In other words, there is a lack of objects with large photometric variability and small values of P. This suggests that the screens do not have a spherically symmetric distribution, but must be roughly confined to the disk, possibly physically related to it.

If screens can form in all HAe stars, then about 1/2 of them (those seen at $\theta \gtrsim 45^o$) should be UXORs, i.e., have irregular minima due to variable circumstellar extinction. Herbst & Shevchenko (1999) list the range of V for a sample of about 80 Herbig AeBe stars, mostly from the ROTOR program of photometric monitoring carried out in Uzbekistan. The observed range of V is greater than 1 mag for about 1/2 of them. Van den Ancker et al. (1998) collected Hipparcos data on HAe variability, covering a much shorter time interval than those in Herbst and Shevchenko, and found 9 stars out of 28 with $\Delta V \gtrsim 0.5$ mag, and 11 with $\Delta V \lesssim 0.1$ mag. These results are roughly consistent with our predictions, but both samples have limited statistical value (selection criteria, time coverage).

4.4. The obscuring screen

The model we propose does not make any specific assumption on the origin and properties of the obscuring screens except for their reddening law. There are however a few points that can be made, which can help in better understanding their nature.

The deep minima of UXORs are caused by rather optically thick dust, with $\tau_V \sim 3$–5. The obscuration caused by such a screen is total only in the blue, while in I we estimate that about 1/2 of the observed radiation is due to the star, and 1/2 is radiation scattered by the disk. The screen, at least at the time of deep minima, must have a core+halo structure, since for any given event the star fades and recovers slowly, with typical timescales of several days. Voshchinnikov & Grinin (1991) in their study of two minima of WW Vul derive a core radius and mass of 0.05–0.15 AU and $10^{19} - 10^{20}$ g of dust respectively, and a halo radius about three times larger.

The characteristics of the polarimetric and photometric variations of UXORs allow us to set some constraints on the projected size of the screen. A minimum radius $\sim R_\star$ is set by the fact that it is very difficult to account for the large values of the

observed P if the screen is smaller in projection than the stellar surface.

Could the screen be much larger than the star? A large screen will occult the inner disk, reducing the fraction of the radiation scattered by the disk we receive, and also, if its optical depth is large enough, obscuring part of the infrared emission of the disk itself. However, there is a compensation effect, because an increasingly larger cloud will intercept an increasingly larger fraction of the stellar radiation (see Appendix), which will be in part scattered and in part re-emitted at infrared wavelengths. Detailed models are needed, but it is clear that, in order to better understand this issue, one needs to understand the infrared variability of UXORs. At present, the observations are very scarce. The only existing near-IR variability study we know of concerns UX Ori, where Hutchinson et al. (1994) report an increase of ~ 0.9 mag in M and ~ 0.5 mag in N occurring simultaneously with a decrease in the visual of $\Delta V \sim 0.3$ mag. Simultaneous J,H,K observations did not show any variation. The infrared variability of UXORs is obviously an area where one can expect much progress in the future.

The origin and evolution of the screen cannot be constrained by our analysis. However, the fact that all the observational properties of UXORs (SEDs, millimeter interferometry data, behaviour of the visual photometric and polarimetric variability) are consistent with the presence of an optically thick, rather massive circumstellar disk, as observed in the lower mass TTS, suggests to look for mechanisms which can give origin to the screens within the disk itself. We find, for example, particularly interesting the possibility that the bulging of the inner disk may vary with time, due to a variable rate of accretion, and occasionally intersect the line of sight between the observer and the star (Bell et al. 1997; Bell 1999). The applicability and implications of such models in the context of Herbig Ae stars need to be explored in a more quantitative way.

5. Summary and conclusions

This paper discusses the photometric and polarimetric variability of UXORs in terms of a model where the central star is surrounded by an optically thick circumstellar disk, with properties similar to those of disks around pre-main–sequence stars. We have been motivated by the fact that similar disks can account for the millimeter fluxes detected in many UXORs and for their IR emission. The light received by the observer is the sum of direct stellar light and of light scattered by the disk into the line of sight. A UXORs minimum is simulated by adding to the system a screen of dust, which sporadically intercepts the line of sight from the observer to the star. If the optical depth of the screen is infinite, only light scattered by the disk can reach the observer.

We consider flared disks such as described by Chiang & Goldreich (1997) and compute the polarization and colors of the observed radiation as a function of the optical depth of the screen using a Monte Carlo code developed by Whitney & Hartmann (1992). We find a remarkably good agreement between our model predictions and the observations of UXORs, as sum-
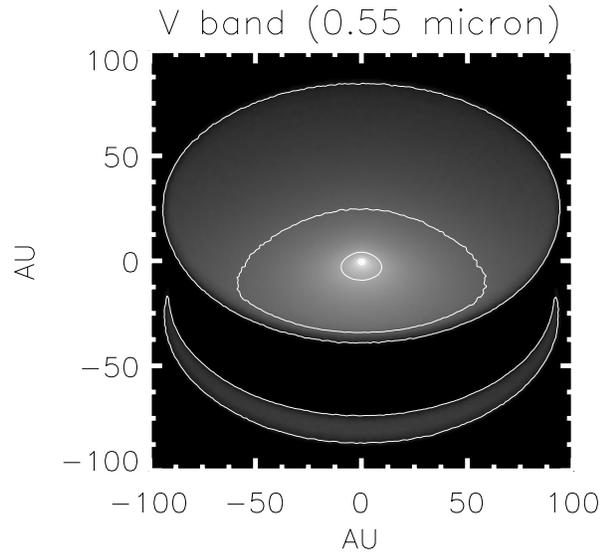
Fig. 9. V image of the CG97 standard disk with $M_D=0.01 M_\odot$ seen during a deep minimum at an inclination $\theta = 60^o$. The contours are 6.7×10^{-8}, 1.7×10^{-6} and 4.2×10^{-5} in units of the V stellar flux per AU^2.

marized in the literature. The results are not sensitive to the disk parameters, as long as the disk intercepts about 20% of the stellar radiation. Although these results do not rule out the possibility that other models can also explain the observations, they prove that disks are comfortably capable of doing so.

A comparison of the model predictions with the observations of UXORs during photometric minima shows that the UXOR phenomenon occurs for systems seen in a well-defined range of inclinations, which we estimate roughly to be between 45° and $65^o - 68^o$. More edge-on disks will intercept the stellar radiation at all times, while more face-on systems cannot reproduce the observed polarization fraction. Hence, the orientation of the disk seems to have an important role. This range of viewing angles however is quite large. If we consider that stars obscured by the outer disk will not be classified as Herbig Ae stars (because they are not optically visible) we expect to have 50% of HAe with disk inclination between 0° and 45°, and 50% between 45° and 67°. Thus, if the phenomenon which causes the screens exists in all systems, we can expect that about 1/2 of the HAe stars should be UXORs, i.e., have deep photometric minima accompanied by a large increase in the polarization fraction.

The nature and origin of the screen remains an open question. The results discussed in this paper help in constraining more precisely their properties. As we have seen, the screens probably have sizes of the order of 1–few stellar radii, optical depth $\tau_V \sim 3$–5, and relatively small grains. We find a good fit to the observations with a MRN distribution with average radius $\sim 0.03 \mu$m. Furthermore, the lack of UXORs with low polarization in deep minima can be understood if the screens are in some way confined in a region close to the disk plane.

Finally, we want to point out that at minimum light the clump is a perfect coronograph, so that it may be possible to image the inner regions of the disk. We show in Fig. 9 the model-predicted

image of our CG97 standard model of mass M_D=0.01 M$_\odot$ seen at an inclination of 60° in V during a deep minimum. The disk is tilted toward the observer, but one can see some scattered light from the edge of its bottom side. The location of the star (which is completely obscured) is in the center. The three contour levels overlayed on the image correspond to flux levels relative to the stellar flux of 6.7×10^{-8}, 1.7×10^{-6}, and 4.2×10^{-5} per AU^2. If we consider, for example, the rather distant UX Ori (d=450 pc, V=9.6 mag) and the Hubble Space Telescope WFPC2 camera (pixel size 0.046$''$), we obtain for the three contours a visual magnitude per pixel of 21.3, 17.8, and 14.3, which is within the sensitivity limits of HST. In this ideal experiment, we could image not only the outer disk but also its inner parts, down to radii of $\sim$ 40 AU. On a closer star, like CQ Tau ($d\sim$ 100 pc) one could resolve the disk down to $\sim$ 10 AU. The best observations of the HAe star AB Aur (d=130 pc; Grady et al. 1999) using STIS on HST can only see the disk at radii larger than $\sim$ 1$''$ (130 AU), due to the presence of the occulting wedge mask.

Appendix A: scattered-light contribution from a spherical cloud

A spherical cloud with radius r_c at a distance d_c from the star will subtend a solid angle, as seen by the star, of

$$\Omega = 2\pi\,(1-\cos\theta_c) \tag{A.1}$$

where $2\theta_c$ is the angle subtended by the cloud. The fraction of stellar light intercepted by the cloud is $\Omega/4\pi$. The cloud reflects a fraction Φ of the incident radiation which varies with α, the angle between incident and reflected flux. Thus, the amount of light reflected into an arbitrary angle α is

$$L_c = \frac{1}{2}\,\Phi(\alpha)\,L_\star\,(1-\cos\theta_c), \tag{A.2}$$

and the flux of the cloud at earth is

$$F_c = 2\pi\,\Phi(\alpha)\,F_\star\,(1-\cos\theta_c), \tag{A.3}$$

or

$$F_c = 2\pi\,\Phi(\alpha)\,F_\star\,\left(1-\frac{d_c}{\sqrt{d_c^2+r_c^2}}\right). \tag{A.4}$$

Let us assume that the cloud is beyond the dust destruction radius (about 10 R$_\star$) and has radius $r_c = 2$R$_\star$. Code & Whitney (1995) calculated phase functions ($\Phi(\alpha)$) for scattering from spherical clouds. For normal ISM dust, at the most optimal scattering angle ($\alpha = 0$), and optimal optical depth ($\tau_c = 0.1$), they give $\Phi(\alpha) = 0.11$. $\Phi(\alpha)$ is at least five times lower for $\tau_c \gtrsim 2$. From Eq. (A.4), one finds $F_c \lesssim 0.003F_\star$ for $\tau_c \sim 2$. Our standard disks scatter $F_d \sim 0.10F_\star$, at least

30 times more than a close-in spherical cloud for realistic values of the parameters. Ignoring the scattering from the cloud should not change the results by any significant amount.

References

Bell K.R., 1999, ApJ 526, 411
Bell K.R., Cassen M.P., Klahr H.H., Henning Th., 1997, ApJ 486, 372
Berdyugin A.V., 1993, Crimean Bull. 87, 107
Berdyugin A.V., Berdyugina S.V., Grinin V.P., Minikulov N.Kh., 1990, SvA 34, 408
Berdyugin A.V., Grinin V.P., Minikulov N.H., 1992, Crimean Bull. 86, 69
Chiang E., Goldreich P., 1997, (CG97), ApJ 490, 368
Chiang E., Goldreich P., 1999, ApJ 519, 279
Code A.D., Whitney B.A., 1995, ApJ 441, 400
Friedemann C., Reimann H.-G., Guertler J., Tóth V., 1993, A&A 277, 184
Friedemann C., Guertler J., Reimann H.-G., 1995, A&A 300,, 195
Gledhill T.M., Scarrott S.M., Wolstencroft R.D., 1995, MNRAS 252, 50
Grady C., Sitko M.L., Russell R.W., et al., 2000, In: Mannings V., Boss A.P., Russell S.R. (eds.) Protostars and Planets IV, University of Arizona Press, Tucson
Grady C., Woodgate W., Bruhweiler F.C., et al., 1999, ApJ 523, L151
Grinin V.P., 1992, Astron. Astrophys. Trans. 3, 17
Grinin V.P., 1994, In: Thé P.S., Pérez M.R., van den Heuvel E.P.J. (eds.) The Nature and Evolutionary Status of Herbig Ae/Be Stars. ASP Conf. Series 62, p. 63
Grinin V.P., Kolotilov E.A., Rostopchina A., 1995, A&AS 112, 457
Grinin V.P., Rostopchina A.N., 1996, Astron. Rep. 40, 171
Herbst W., Shevchenko V.S., 1999, AJ 118, 1043
Kim S.-H., Martin P. G., Hendry P. D., 1994, ApJ 422, 164
Krivova N.A., Il'in V.B., 1997, Astron. Let. 23, 791
Krivova N.A., Il'in V.B., 2000, Icarus 143, 159
Mannings V., Sargent A.I.,, 1997, ApJ 490, 792
Mannings V., Sargent A.I., 2000, ApJ 529, 391
Mathis J.S., Rumpl W., Nordsieck K.H., 1977, ApJ 217, 425 (MRN)
Natta A., Grinin V.P., Mannings V., 2000, In: Mannings V., Boss A.P., Russell S.R. (eds.) Protostars and Planets IV, University of Arizona Press, Tucson
Natta A., Grinin V.P., Mannings V., Ungerechts H., 1997, ApJ 491, 885
Natta A., Prusti T., Neri R., et al., 1999, A&A 350, 541
Reimann H.-G., Guertler J., Friedemann C., Kaeufl H.U., 1997, A&A 326, 271
Rostopchina A., Grinin V.P., Okazaki A., et al., 1997, A&A 327, 145
Ruden S.P., 2000, In: Mannings V., Boss A.P., Russell S.R. (eds.) Protostars and Planets IV, University of Arizona Press, Tucson
van den Ancker M.E., de Winter D., Tjin A Djie H.R.E., 1998, A&A 330, 145
Voshchinnikov N.V., Grinin V.P., 1991, Afz 34, 84
Voshchinnikov N.V., Grinin V.P., Karjukin V.V., 1995, A&A 294, 547
Voshchinnikov N.V., Grinin V.P., Kiselev N.N., Minikulav N.K., 1988, Afz 28, 311
Waters L.B.F.M., Waelkens C., 1998, ARA&A 36, 233
Whitney B.A., Hartmann L., 1992, ApJ 395, 529
Wolstencroft R.D., Scarrott S.M., Gledhill T.M., 1995, Ap&SS 224, 395